Ab initio study of the effect of vacancies on the thermal conductivity of boron arsenide

Nakib Haider Protik, Jesús Carrete, Nebil A. Katcho, Natalio Mingo, and David Broido

Phys. Rev. B **94**, 045207 — Published 28 July 2016

DOI: 10.1103/PhysRevB.94.045207

Ab initio study of the effect of vacancies on the thermal conductivity of boron arsenide

Nakib Haider Protik,[1,*] Jesús Carrete,[2] Nebil A. Katcho,[3] Natalio Mingo,[2] and David Broido[1]

[1] *Department of Physics, Boston College, Chestnut Hill, Massachusetts 02467, USA*
[2] *LITEN, CEA-Grenoble, 17 rue des Martyrs, 38054 Grenoble Cedex 9, France*
[3] *CIC Energigune, Albert Einstein 48, 01510 Miñano, Álava, Spain*

(Dated: July 6, 2016)

Using a first principles theoretical approach, we show that vacancies give anomalously strong suppression of the lattice thermal conductivity, κ, of cubic Boron arsenide (BAs), which has recently been predicted to have an exceptionally high κ. This effect is tied to the unusually large phonon lifetimes in BAs and results in a stronger reduction in the BAs κ than occurs in diamond. The large bond distortions around vacancies cannot be accurately captured using standard perturbative methods and are instead treated here using an ab initio Green function approach. As and B vacancies are found to have similar effects on κ. In contrast, we show that commonly used mass disorder models for vacancies fail for large mass ratio compounds such as BAs, incorrectly predicting much stronger (weaker) phonon scattering when the vacancy is on the heavy (light) atom site. The quantitative treatment given here contributes to fundamental understanding of the effect of point defects on thermal transport in solids and provides guidance to synthesis efforts to grow high quality BAs.

PACS numbers: 63.20.kg, 63.20.kp, 61.72.-y, 63.20dk

I. INTRODUCTION

Cubic boron arsenide (BAs) has recently been predicted to have an ultrahigh lattice thermal conductivity, κ, comparable to that of diamond[1,2]. This has led to an increased interest in the material because of the novel way in which its high κ is achieved, and because of its potential for use in thermal management applications. To date, experimental verification of the high κ of BAs has proved challenging because of the difficulty in growing high quality single crystal samples[3,4]. In particular, in Ref. 3, the presence of high As vacancy concentrations was suspected from chemical vapor transport synthesis. Therefore it is of importance to accurately calculate the effect of As vacancies on the BAs κ.

BAs is a semiconductor with energy gap of about 1.5 eV[5]. Thus, heat is carried primarily by phonons. The standard method of studying the effect of point defects such as vacancies on phonon thermal transport is the Born approximation[6], which treats the defect in lowest-order perturbation theory. However, vacancies represent large perturbations, making the Born approximation questionable. Furthermore, simple theories have treated vacancies as effective on-site mass defects[7]. For large mass ratio compounds, such theories would predict much larger phonon scattering from vacancies on the heavy atom site compared to those on the light atom site. Recently, that view has been called into question. Instead, it has been shown that vacancies should be treated only as bond defects since a change in the mass of a non-interacting atom does not perturb the dynamics of the system[8].

In this work, we calculate the phonon-vacancy scattering rates and lattice thermal conductivity of BAs for both As and B vacancies as a function of vacancy concentration using a Green's (Green)[9] function based T-matrix approach[8,10,11], which treats the perturbation to all orders. Section II describes the first principles theory of phonon thermal transport. In Section III, the T-matrix treatment of phonon-vacancy scattering is given. Section IV describes the computational details, while section V presents the results along with discussion. Section VI summarizes our findings.

II. AB INITIO PHONON HEAT TRANSPORT

In semiconducting and insulating materials phonons are the main carriers of heat. Three-phonon scattering and phonon-defect scattering typically limit the lattice thermal conductivity around and above room temperature[12]. The non-equilibrium phonon distribution resulting from an applied temperature gradient in a material is described through the Peierls-Boltzmann transport equation (BTE):

$$\mathbf{v}_\lambda \cdot \nabla T \frac{\partial n_\lambda}{\partial T} = \left(\frac{\partial n_\lambda}{\partial t}\right)_{\text{collisions}} \tag{1}$$

where $\lambda \equiv (\mathbf{q}, s)$ labels the phonon mode with wavevector $\mathbf{q}$ and polarization s, n_λ is the non-equilibrium distribution of phonons, $\mathbf{v}_\lambda$ is the phonon group velocity, and ∇T is the applied temperature gradient. Here, the left hand side term represents phonon drift due to the applied temperature gradient, and the right hand side is due to phonon scattering.

In our first principles approach, we take the temperature gradient, ∇T, to be small. The non-equilibrium phonon distribution can then expanded in powers ∇T and, retaining only up to linear order in ∇T, it can be written as $n_\lambda = n^0_\lambda + \left(-\partial n^0_\lambda / \partial T\right) \mathbf{F}_\lambda \cdot \nabla T$, where n^0_λ is the

Bose distribution. In this limit, the BTE is also linearized in ∇T and can be recast as $\mathbf{F}_\lambda = \tau_\lambda^0 (\mathbf{v}_\lambda + \mathbf{\Delta}_\lambda)$. Here, $1/\tau_\lambda^0$ is the total scattering rate in mode λ, which includes intrinsic phonon-phonon scattering and scattering from defects, and $\mathbf{\Delta}_\lambda$ is a linear function of $\mathbf{F}_\lambda$. Explicit definitions of these quantities are given in Refs. 13 and 14. The three-phonon rates are given by Eq. 4 in Ref. 13; isotopes are treated as mass defects, and the phonon-isotope scattering rates in the Born approximation can be expressed in closed form for binary cubic compounds[15]:

$$\frac{1}{\tau_\lambda^{\text{iso}}} = \frac{\pi}{6N} \sum_k g_k |\hat{e}_k^\lambda|^2 D_k(\omega_\lambda) \tag{2}$$

where $D_k(\omega_\lambda) = \sum_{\lambda'} |\hat{e}_k^{\lambda'}|^2 \delta(\omega_\lambda - \omega_{\lambda'})$ is the partial phonon density of states of the k^{th} atom in the unit cell, and

$$g_k = \sum_s f_{sk} \left(\frac{\Delta M_{sk}}{\overline{M}_k} \right)^2 \tag{3}$$

is the mass variance parameter for that atom, with $\Delta M_{sk} \equiv M_{sk} - \overline{M}_k$. In these equations, N is the number of unit cells in the crystal, $(2\pi)^{-1}\omega_\lambda$ and $\hat{e}_k^\lambda$ are the phonon frequency and eigenvector in mode λ, f_{sk} and m_{sk} are the concentration and the mass of the s^{th} type of isotope on the k^{th} atom and $\overline{m}_k$ is the average mass of species k atoms. The thermal conductivity tensor is given by:

$$\kappa^{\alpha\beta} = \frac{k_B}{V} \sum_\lambda \left(\frac{\hbar\omega_\lambda}{k_B T} \right)^2 n_\lambda^0 (n_\lambda^0 + 1) v_\lambda^\alpha F_\lambda^\beta \tag{4}$$

where α and β are Cartesian components, k_B is the Boltzmann constant and V is the crystal volume. For cubic compounds, the thermal conductivity is a scalar: $\kappa \equiv \kappa^{\alpha\alpha}$.

III. PHONON-VACANCY SCATTERING

The phonon modes are obtained from the dynamical equation

$$\omega^2 u_{i\alpha} = \sum_{j\beta} \frac{K_{i\alpha,j\beta}}{\sqrt{M_i M_j}} u_{j\beta} \tag{5}$$

where M_i is the mass of the i^{th} atom, $u_{i\alpha}$ is the atomic displacement of the i^{th} atom in the direction α, and $K_{i\alpha,j\beta}$ are the harmonic interatomic force constants (IFCs). In general, point defects introduce two perturbation potentials: V^{M} and V^{K}, representing the mass and IFC perturbations. The mass perturbation for a defect at defect site i is: $V^{\text{M}}_{i\alpha,j\beta} = -\omega^2 (M_i' - M_i) \delta_{ij} \delta_{\alpha\beta} / M_i$, where the primed mass is the mass of the defect. Note that this type of perturbation acts only at the defect site. In contrast, the bond perturbation extends over a region around the defect site. This perturbation is:

$$V^{\text{K}}_{i\alpha,j\beta} = \frac{\left(K'_{i\alpha,j\beta} - K_{i\alpha,j\beta} \right)}{\sqrt{M_i M_j}} \tag{6}$$

where $K'_{i\alpha,j\beta}$ gives the harmonic force constant between sites i and j after the system has relaxed around the defect. When calculating V^{M} and V^{K} from first principles, care should be taken that the force constants satisfy translational and rotational invariance. This can be enforced by slight modification of the interatomic force constants (IFCs), as shown in Ref. 8.

Vacancy defects are commonly treated within the Born approximation and as on-site defects characterized by an effective mass perturbation that includes both mass and bond perturbations[7,16–18]. For example, in the model of Ratsifaritana and Klemens (RK)[7,17,18], the vacancy perturbation is taken to be:

$$V^{\text{M}}_{i\alpha,j\beta} + V^{\text{K}}_{i\alpha,j\beta} = -\omega^2 \left(2 + \overline{M}_i / \overline{M} \right) \delta_{ij} \delta_{\alpha\beta} \tag{7}$$

where the 2 estimates the effect from broken bond linkages, $\overline{m}_i$ is the mass of the removed atom on unit cell site i and $\overline{M}$ is the average atomic mass. Note that this expression depends explicitly on the mass of the removed atom, which has profound implications for large mass ratio compounds such as BAs, as discussed below.

However, treating a vacancy as a mass defect is conceptually wrong. In a lattice the presence of an atom is felt by its interactions with its neighbors. Creation of a vacancy, therefore, is equivalent to the removal of all the interactions of the rest of the crystal with the atom to be removed. This is true regardless of the mass of the atom. Therefore having a non-zero V^{M} in the case of a complete vacancy is incorrect. Quantitative results in favor of this argument has been made in Ref. 8 for the case of diamond. The discussion in the paragraph above highlights the fact that there is an additional important difference for large mass ratio compounds.

The phonon-vacancy scattering cross section, σ, is obtained by solving the Lippmann-Schwinger equation[19] and is given in our case by[8,10,11]

$$\sigma_\lambda = \frac{\Omega_s \pi}{\omega_\lambda v_\lambda} \sum_{\lambda'} \left| \langle \lambda' | T^+(\omega_\lambda^2) | \lambda \rangle \right|^2 \delta \left(\omega_{\lambda'}^2 - \omega_\lambda^2 \right) \tag{8}$$

where Ω_s is the supercell volume into which phonon eigenstate $|\lambda\rangle$ is normalized and T^+ is known as the T-matrix given by

$$T^+ = \left(I - V G_0^+ \right)^{-1} V \tag{9}$$

where I is the identity matrix, V is the perturbation matrix and G_0^+ is the retarded, unperturbed Green function for phonons given by:

$$G^+_{0,ij}(\omega^2) = \lim_{z \to \omega^2 + i0} \sum_\lambda \langle i|\lambda\rangle \langle \lambda | j \rangle \left(z - \omega_\lambda^2 \right)^{-1} \tag{10}$$

where $|i\rangle, |j\rangle$ represent displacements in the i, j lattice degrees of freedom.

The expansion of Eq. 9 in the perturbation, V, gives us the Born series:

$$T^+ = V + VG_0^+V + VG_0^+VG_0^+V + ... \approx V \qquad (11)$$

where the right-hand side of Eq. 11 defines the typically used first Born approximation.

From σ the phonon-vacancy scattering rate is obtained as $1/\tau_\lambda^{\rm vac} = f v_\lambda \sigma_\lambda / V_0$ where f is the volume fraction of vacancies and V_0 is the volume per atom in the pristine lattice. Here, it is assumed that the vacancies are randomly distributed throughout the crystal and that the vacancy concentration is low enough so that each vacancy behaves as an independent scattering center. We note that the vacancy concentrations considered here are less than 0.2% corresponding to less than one in every 500 atoms. For such dilute concentrations, effects associated with proximity of multiple vacancies such as coherent scattering of phonons should be negligible. The phonon-vacancy scattering rates are used along with the phonon-isotope scattering rates (Eqs. 2, 3) and the phonon-phonon scattering rates to construct the total scattering rates, which are used in an iterative solution of the phonon BTE[14].

Below we compare the results of three approaches to treat vacancies: i) Using the exact T-matrix approach, treating the vacancy as a bond perturbation in Eq. (9), $V = V^{\rm K}$, evaluated to all orders; ii) Using the Born approximation and treating the vacancy as a bond perturbation: $T^+ = V^{\rm K}$; iii) Using the RK model, which uses the Born approximation and uses Eq. 7 as the mass perturbation; iv) Same as iii but treating the perturbation using the full T-matrix. The comparisons of these different models are given in Fig. 6.

IV. COMPUTATIONAL DETAILS

Our first principles approach involves computing the second and third order interatomic force constants (IFCs) using the finite displacement method with the VASP[20–23] implementation of density functional theory (DFT) using the PAW pseudopotentials[24,25] in the PBE[26,27] approximation. Helper pre- and post-processing softwares phonopy[28,29] and thirdorder.py[13,14] are used to create the finite displacements in a $4 \times 4 \times 4$ supercell (128 atoms), and also to read-off the IFCs. The DFT run is carried out on a $2\times2\times2$ Γ-centered Monkhorst-Pack q-grid. The energy cut-off is set at 398 eV. For the pristine lattice, the relaxed BAs lattice constant is $a = 4.82$ Å, slightly larger than the measured value of 4.78 Å in Ref. 3. Here we consider the two cases of single As and single B vacancies. After the creation of each vacancy, the surrounding atom positions are relaxed, fixing the supercell volume to that of the pristine supercell. The acoustic sum rule is imposed in the computation of both the pristine and defected supercell harmonic IFCs.

The harmonic IFCs for the pristine and the defected system are used to calculate the perturbation matrix, $V^{\rm K}$ using Eq. 6. Since anharmonic interactions are weak, the vacancy is represented sufficiently well by the change in the harmonic IFCs only. The changes in the harmonic IFCs are considered for a cluster radius of 6.1 Å around the vacancy, taking into account the first- and second-nearest neighbor interactions for the atoms in the six nearest shells around the vacancy site. From the perturbation matrix, σ is calculated on a $28 \times 28 \times 28$ k-grid. The phonon-vacancy scattering rates for each vacancy concentration are then combined using Matheissen's rule with phonon-phonon and phonon-isotope scattering rates determined from ShengBTE[14,30] . The total scattering rates are used in an iterative solution of the linearlized Boltzmann equation and a converged κ is obtained using the ShengBTE platform.

V. RESULTS AND DISCUSSIONS

The phonon dispersions of BAs and diamond are shown in Figs. 1a and 1b. These figures illustrate different features that help give each material its high intrinsic thermal conductivity. In BAs, the large frequency gap between acoustic (a) and optic (o) phonons ($a - o$ gap) prevents the $a + a \leftrightarrow o$ (aao) scattering since energy cannot be conserved. Also, the phase space for $a + a \leftrightarrow a$ (aaa) scattering is severely restricted owing to the bunching of the acoustic branches coupled with a theorem that says that three phonons from the same acoustic branch cannot conserve both momentum and energy[31]. These two vibrational properties along with the isotopic purity of the heavy As atom give BAs an ultrahigh intrinsic κ of over 3000 $\rm Wm^{-1}K^{-1}$ at room temperature. In contrast, the light carbon atoms and strong covalent bonding give diamond the high phonon frequency scale contributing to its high κ.

The distortions of bond lengths and bond angles around As and B vacancies are shown in Figs. 2a and 2b. The maximum change in bond length(angle) is 2.5(3.3)% of that of the pristine case for As vacancies and 0.42(0.96)% for B vacancies and occurs at the nearest and second nearest neighbor sites from the As vacancy, and at the second nearest neighbor sites from the B vacancy. In the case of diamond these numbers are 3.3% and 3.7%, respectively[8]. The distortions around the As and B vacancies extend up to about 5 Å from the defect site, a distance that is much smaller than the $4\times4\times4$ supercell size of about 13.6 Å. Nevertheless, we have performed calculations for As vacancies in BAs with a $5 \times 5 \times 5$ supercell (250 atoms). As seen in Figs. 2a and 2b, bond length and bond angle distortions for this case are almost exactly the same as those for the $4\times4\times4$ supercell justifying its use for all further calculations described below.

Fig. 3 shows the phonon-phonon scattering rates (solid black squares) and the phonon-vacancy scattering rates for 0.01 and 0.1% As vacancy concentrations in BAs in

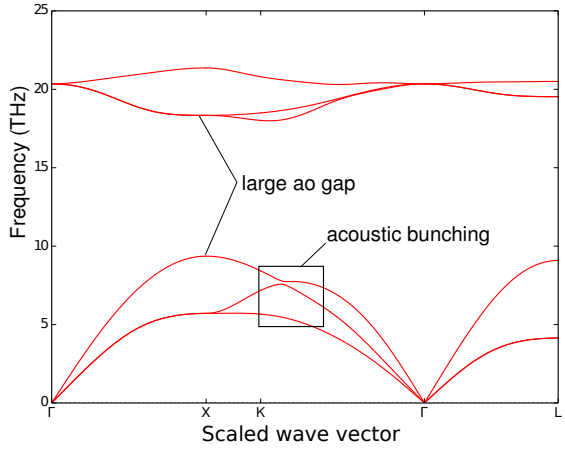

(a)

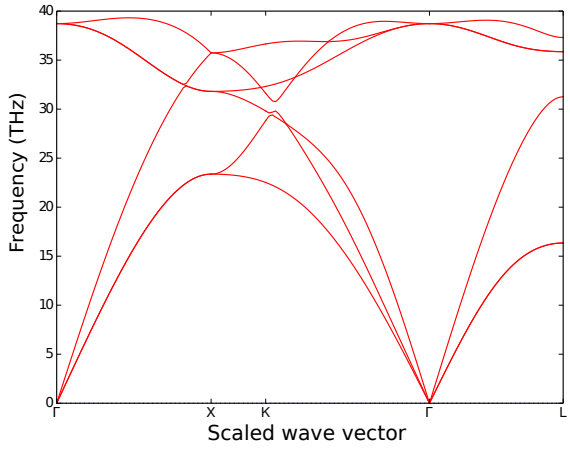

(b)

FIG. 1. Phonon Dispersions of BAs (a) and diamond (b) along high symmetry directions.

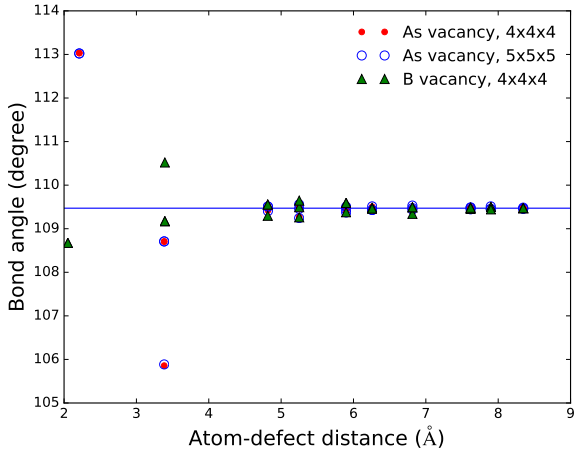

(a)

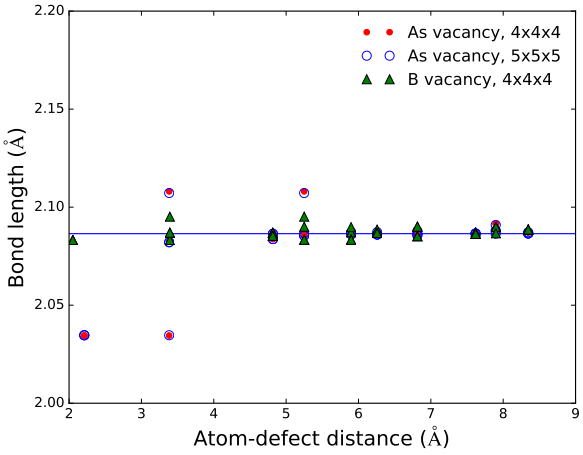

(b)

FIG. 2. Distortion of bond (a) length and (b) angle for As and B vacancies. Blue lines represent the relaxed bond length, 2.09 Å, and angle, 109.5°, for the pristine crystal, respectively. The data points corresponding to As vacancy for the $4\times4\times4$ and $5\times5\times5$ supercells coincide almost perfectly.

the Born approximation (open and solid blue circles) and T-matrix method (open and solid red triangles) in the longitudinal acoustic (LA) branch. Other branches show similar behavior. In the Born approximation the scattering rates are significantly underestimated except at high frequencies where they exceed the scattering rates calculated in the T-matrix formalism. Similar behavior was found previously for diamond[8]. Note the dip in the phonon-phonon scattering rates in the mid-high frequency range, which is due to the suppressed phase space for phonon-phonon scattering from the large $a-o$ gap and the acoustic bunching shown in Fig. 1a. It is this frequency region that gives the largest contribution to the vacancy-free BAs κ. This is shown by the black dotted curve in Fig. 4. From this figure, we see that when the phonon-vacancy scattering rates are comparable to or larger than the phonon-phonon scattering rates, a large suppression of κ is expected.

Fig. 5 shows the κ .vs. As vacancy concentration within the Born and T-matrix approaches. Surprisingly, the two results are quite close for As vacancy concentrations up to about 0.01%. This fortuitous agreement is in fact a consequence of two failures of the Born approximation: It underestimates the scattering rates at low frequency and overestimates them at high frequency, as seen in Fig. 3. For concentrations below 0.01%, these two errors cancel. This is seen in the $\kappa(\nu)$ curves for 0.01% in Fig. 4 which shows similar areas under the red (T-matrix) and blue (Born) dashed curves. With increasing As vacancy concentration above 0.01%, the phonon-vacancy scattering rates become much stronger than the phonon-phonon scattering rates where the phonon-phonon scattering shows a dip. Then, the larger T-

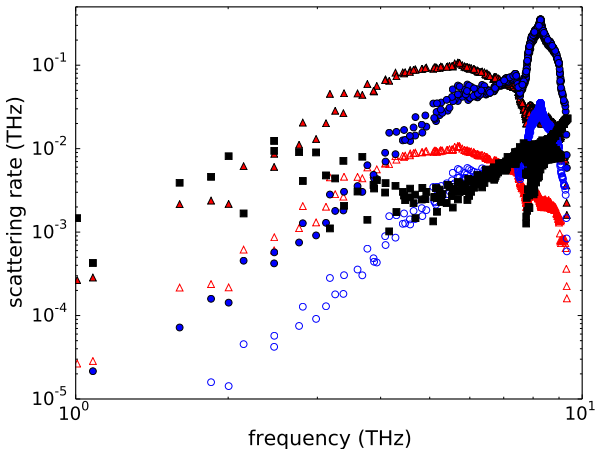

FIG. 3. Three-phonon scattering rates at 300K for the LA phonon branch in BAs as a function of phonon frequency (solid black squares), compared with the scattering rates of phonons from As vacancies. Open (solid) blue circles give Born approximation results for 0.01% (0.1%) As vacancies, while the corresponding T-matrix results are shown by the open and solid red triangles.

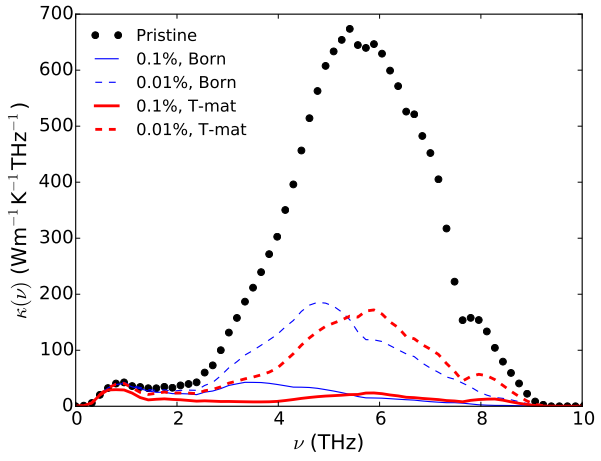

FIG. 4. The contribution to κ at 300K as a function of frequency, ν, where $\kappa = \int \kappa(\nu) d\nu$. The black dotted curve gives $\kappa(\nu)$ for vacancy-free BAs for naturally occurring isotope mix (19.9% ^{10}B, 80.1% ^{11}B); the thin blue dashed and solid curve gives Born approximation results for 0.01 and 0.1% As vacancies, respectively, while the thick red dashed and solid curves give the corresponding results obtained using the T-matrix approach.

matrix scattering rates are seen in Fig. 4 to give a larger reduction in κ than in the Born approximation (compare red and blue solid curves). This difference becomes about a factor of two for 0.2% As vacancies.

As noted above, previous models to estimate the effect of vacancies on the lattice thermal conductivity use the Born approximation with an on-site effective mass

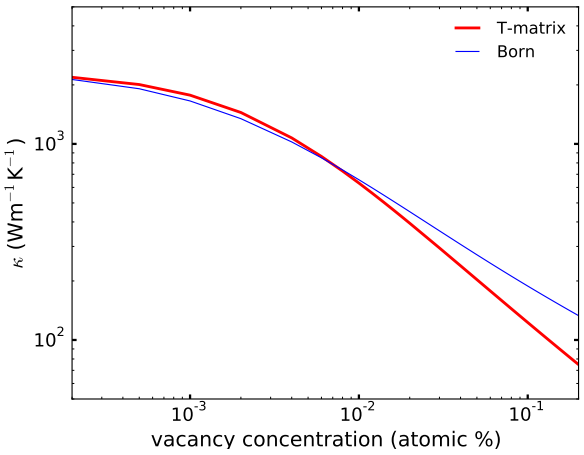

FIG. 5. The room temperature thermal conductivity of BAs as a function of As vacancy concentration in the Born approximation (thin blue curve) and using the T-matrix method (thick red curve).

perturbation[7,16–18]. This corresponds to Eqs. 7 and 11 inserted in Eq. 8. The resulting thermal conductivities .vs. As and B vacancy concentrations (green solid and dashed curves) are plotted in Fig. 6 along with the corresponding results from the full T-matrix calculations (red curve and red points). Note that the RK model significantly underestimates the effect of the light atom (B) vacancy and overestimates the effect of the heavy atom (As) vacancy. This is a general feature of large mass ratio compounds, which has two underlying reasons. First, the mass perturbation itself is larger for the heavy atom: In BAs, the value of the parentheses in Eq. 7 is 3.75 for As vacancies, 1.7 times larger than the 2.25 for B vacancies. Secondly, the heavy atom dominates the vibrational motion of the heat-carrying acoustic modes[15,31], e.g. the phonon eigenvector components for As are much larger than those for B throughout the Brillouin zone.

The blue line and blue triangles in Fig. 6 show results using the RK mass perturbation, Eq. 7, in the full T-matrix scattering crossection. Since B vacancies give a weak mass-defect perturbation, the Born approximation and T-matrix results are almost the same. In contrast, for As vacancies the T-matrix result shows that the actual phonon-vacancy scattering is weaker than estimated by the Born approximation. Here, since the mass perturbation is proportional to ω^2, the Born approximation fails badly in the high frequency range. Nevertheless, even the T-matrix treatment still incorrectly predicts an order of magnitude smaller κ for As vacancies compared to B vacancies at a concentration of 0.2%. Thus, the failure of the RK model in large mass ratio compounds stems both from treating the vacancy as a mass defect and from the failure of the Born approximation in treating large perturbations.

Given the differences in the distortions of atoms around

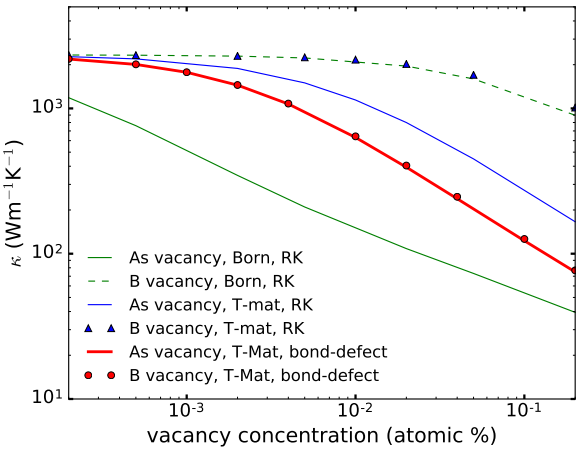

FIG. 6. The room temperature thermal conductivity of BAs as a function of atomic percent As and B vacancies using the T-matrix (thick red line and red circles) method compared to the corresponding results for As (thin green solid curve) and B (green dashed curve) obtained from the RK model treated in the Born approximation. Result for RK model treated in the T-matrix approach for As is given by the blue line while blue triangles are for B vacancy.

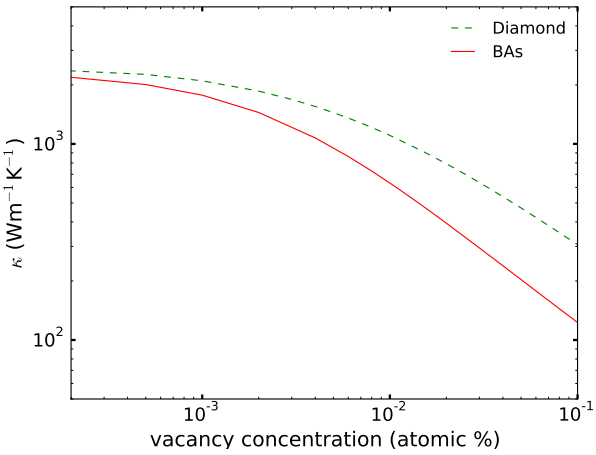

FIG. 7. The room temperature thermal conductivities of BAs and diamond as functions of atomic percent of As and C vacancies, respectively.

As and B vacancies seen in Figs. 2a and 2b, it is somewhat surprising that the T-matrix results for As and B vacancies seen in Fig. 6 are almost the same throughout the range of vacancy concentrations considered. In fact, the scattering rates for As and B vacancies do show modest differences, but effects on $\kappa(\nu)$ tend to cancel over the full frequency range of the acoustic phonons.

High quality diamond, designated type-II a reflecting low concentrations of nitrogen defects, is also thought to have very low vacancy concentrations; the observed ultrahigh thermal conductivities[32–34] could not be achieved otherwise. The reduction in κ introduced by irradiating type-II a diamond was studied by Burgemeister and Ammerlaan[35], and good agreement with this data was recently achieved from first principles calculations[8], demonstrating that such calculations can properly capture the interplay between phonon-phonon and phonon-vacancy scattering. Since BAs is predicted to have roughly the same room temperature κ as diamond, it is then natural to compare the effects of vacancies on the thermal conductivities of these two materials. Fig. 7 shows that BAs is more strongly affected by the presence of vacancies than is diamond. For example, at 0.1% vacancy concentration, the natural BAs κ is reduced from the calculated pristine value of about 2300 Wm^{-1}K^{-1} to 120 Wm^{-1}K^{-1}, a reduction of 95%. In natural diamond, on the other hand, κ is reduced by 88% from the pristine value of about 2500 Wm^{-1}K^{-1} to 300 Wm^{-1}K^{-1}. At 0.01% defect concentrations, these numbers are 73% and 55%, respectively for BAs and diamond. As mentioned above, for BAs, the elimination of scattering between acoustic and optic phonons and small phase space for scattering between acoustic phonons in the mid-high range of the acoustic phonon spectrum gives very weak scattering rates and correspondingly large contributions to the BAs κ over this relatively narrow frequency range. For large vacancy concentrations, the phonon-vacancy scattering is strong over this frequency range, which then has a profound effect on κ. For diamond, this is not the case. Instead, the κ contributions extend over a wide frequency range, and the phonon-vacancy scattering is therefore less effective at reducing κ. This result is consistent with the fact that the phonon mean free paths contributing to the intrinsic BAs κ are quite large, in the $1-3\mu$m range, while those for diamond are smaller, mostly below 1μm^2. Consequently, to achieve room temperature κ in BAs over 1000 Wm^{-1}K^{-1}, the target As vacancy atomic percent should be no more than 0.004%. This translates to an As vacancy concentration of about 3×10^{18} cm^{-3}.

It is interesting to compare the temperature dependence of the κ for BAs and diamond for fixed vacancy concentration. In diamond, phonon-phonon scattering around and above room temperature has a strong temperature dependence. This occurs because the diamond frequency scale is high, and as T increases above 300K, scattering of the heat-carrying acoustic phonons by optic phonons becomes stronger. In contrast, in BAs three-phonon scattering between the heat-carrying acoustic phonons and optic phonons is quite weak because there is no phase space for *aao* processes and only a very small phase space for *aoo* processes. As a result, the BAs κ shows a weaker T dependence than that of diamond, as seen in Fig. 8 for the case of 0.01% As vacancies. Thus, for example, at 300 K the κ of BAs is about 40% that of diamond, while at 900 K, it is almost 75% that of diamond.

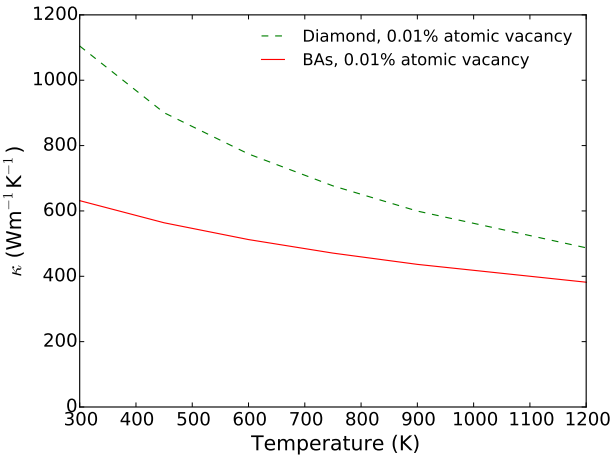

FIG. 8. Temperature dependence of the thermal conductivity of BAs (diamond) for 0.01% As (C) vacancies.

VI. CONCLUSIONS

The effect of As vacancies on the lattice thermal conductivity, κ, of cubic boron arsenide has been investigated using an ab initio approach that treats the vacancy to all orders in perturbation theory. The large contribution to the defect-free BAs κ coming from a narrow range of frequencies is suppressed for large As vacancy concentration leading to larger κ reduction compared to that for diamond. However, the T-dependence of the κ of BAs is shown to be weaker than that of diamond making the effect of vacancies on these two ultrahigh κ materials more comparable at higher T.

The physically-motivated treatment of vacancies solely as bond defects gives almost the same κ reduction for B as for As vacancies. In contrast, the common treatment of vacancies as mass defects predicts a sensitive dependence of phonon-vacancy scattering on the mass of the constituent atom and gives much too large suppression of κ with As vacancy concentration. We note that this difference provides a means of testing experimentally the validity of mass defect models for vacancies. If two samples of the same large mass ratio binary compound could be grown in a controlled way so that each sample had the same vacancy concentration of one or the other constituent atom, then if a similar reduction in κ occurs, this would discount the mass defect models.

The Born approximation, commonly used to treat phonon-defect scattering, is demonstrated to underestimate the reduction in the BAs κ when the vacancy is treated as a bond defect and to overestimate this reduction when the vacancy is treated as a mass defect. This failure highlights the need to treat vacancies in large mass ratio compounds using the full T-matrix approach presented here.

Despite the strong effect on the BAs κ due to vacancies, high κ can still be achieved with advances in synthesis approaches. For vacancy concentrations of below 3×10^{18} cm^{-3}, the calculated room temperature BAs κ is over 1000 Wm^{-1}K^{-1}. We note that in GaN, a large mass ratio compound mirroring BAs across the group IV column of the periodic table, Ga vacancy concentrations of less than a few times 10^{16} cm^{-3} have been achieved[36]. If similarly low As vacancy concentrations could be achieved in BAs, its ultrahigh thermal conductivity should remain unaffected.

ACKNOWLEDGEMENTS

N.H.P. and D.B. acknowledge support from the National Science Foundation under grant No. 1402949, from the Office of Naval Research MURI, grant No. *N*00014-16-1-2436, and from the Pleiades computational cluster of Boston College. N.H.P. also acknowledges help from Matthew Heine with VASP calculations. J.C. and N. M. acknowledge support from European Union's Horizon 2020 Research and Innovation Programme [grant number 645776 (ALMA)], the M-Era program through project ICETS, and ANR through project Carnot SIEVE.

* nakib.protik@bc.edu

[1] L. Lindsay, D. A. Broido, and T. L. Reinecke, Physical Review Letters **111**, 025901 (2013).
[2] D. A. Broido, L. Lindsay, and T. L. Reinecke, Physical Review B **88**, 214303 (2013).
[3] B. Lv, Y. Lan, X. Wang, Q. Zhang, Y. Hu, A. J. Jacobson, D. Broido, G. Chen, Z. Ren, and C.-W. Chu, Applied Physics Letters **106**, 074105 (2015).
[4] J. Kim, D. A. Evans, D. P. Sellan, O. M. Williams, E. Ou, A. H. Cowley, and L. Shi, Applied Physics Letters **108**, 201905 (2016).
[5] S. Wang, S. F. Swingle, H. Ye, F.-R. F. Fan, A. H. Cowley, and A. J. Bard, Journal of the American Chemical Society **134**, 11056 (2012).
[6] J. Sakurai, *Modern Quantum Mechanics* (Wesley Publishing Company, 1994).
[7] P. Klemens, High Temperatures - High Pressures **17**, 41 (1985).
[8] N. A. Katcho, J. Carrete, W. Li, and N. Mingo, Physical Review B **90**, 094117 (2014).
[9] M. C. M. Wright, Nature Physics **2**, 646 (2006).
[10] A. Kundu, N. Mingo, D. A. Broido, and D. A. Stewart, Physical Review B **84**, 125426 (2011).
[11] N. Mingo, K. Esfarjani, D. A. Broido, and D. A. Stewart, Physical Review B **81**, 045408 (2010).
[12] J. M. Ziman, *Electrons and phonons: the theory of transport phenomena in solids* (Oxford University Press, 1960).
[13] W. Li, L. Lindsay, D. A. Broido, D. A. Stewart, and N. Mingo, Physical Review B **86**, 174307 (2012).

[14] W. Li, J. Carrete, N. A. Katcho, and N. Mingo, Computer Physics Communications **185**, 17471758 (2014).
[15] S.-i. Tamura, Physical Review B **30**, 849 (1984).
[16] V. Gallina and M. Omini, Physica Status Solidi (b) **7**, 29 (1964).
[17] C. Ratsifaritana, *Phonon Scattering in Condensed Matter, ed. HJ Maris* (Plenum Press, New York, 1980) pp. 259–262.
[18] C. Ratsifaritana and P. Klemens, International Journal of Thermophysics **8**, 737 (1987).
[19] B. A. Lippmann and J. Schwinger, Physical Review **79**, 469 (1950).
[20] G. Kresse and J. Hafner, Physical Review B **47**, 558 (1993).
[21] G. Kresse and J. Hafner, Physical Review B **49**, 14251 (1994).
[22] G. Kresse and J. Furthmüller, Physical Review B **54**, 11169 (1996).
[23] G. Kresse and J. Furthmüller, Physical Review B **54**, 11169 (1996).
[24] P. E. Blöchl, Physical Review B **50**, 17953 (1994).
[25] G. Kresse and D. Joubert, Physical Review B **59**, 1758 (1999).
[26] J. P. Perdew, K. Burke, and M. Ernzerhof, Physical Review Letters **77**, 3865 (1996).
[27] K. Burke, J. P. Perdew, and M. Ernzerhof, The Journal of Chemical Physics **109**, 3760 (1998).
[28] A. Togo and I. Tanaka, Scripta Materialia **108**, 1 (2015).
[29] A. Togo, F. Oba, and I. Tanaka, Physical Review B **78**, 134106 (2008).
[30] W. Li, N. Mingo, L. Lindsay, D. A. Broido, D. A. Stewart, and N. A. Katcho, Physical Review B **85**, 195436 (2012).
[31] M. Lax, P. Hu, and V. Narayanamurti, Physical Review B **23**, 3095 (1981).
[32] D. G. Onn, A. Witek, Y. Z. Qiu, T. R. Anthony, and W. F. Banholzer, Physical Review Letters **68**, 2806 (1992).
[33] J. R. Olson, R. O. Pohl, J. W. Vandersande, A. Zoltan, T. R. Anthony, and W. F. Banholzer, Physical Review B **47**, 14850 (1993).
[34] L. Wei, P. K. Kuo, R. L. Thomas, T. R. Anthony, and W. F. Banholzer, Physical Review Letters **70**, 3764 (1993).
[35] E. A. Burgemeister and C. A. J. Ammerlaan, Physical Review B **21**, 2499 (1980).
[36] J. Oila, J. Kivioja, V. Ranki, K. Saarinen, D. C. Look, R. J. Molnar, S. S. Park, S. Lee, and J. Han, Applied Physics Letters **82**, 3433 (2003).